Organophilization of a Brazilian Mg-montmorillonite without prior sodium activation

MANOELLA SILVA CAVALCANTE[1,*], SIMONE PATRÍCIA ARANHA PAZ[2], RÔMULO SIMÕES ANGÉLICA[1], EDSON NORYUKI ITO[3] AND ROBERTO FREITAS NEVES[1]

[1] *Programa de Pós-Graduação em Geologia e Geoquímica, Instituto de Geociências, Universidade Federal do Pará, Campus do Guamá, 66075-110, Belém, Pará, Brazil*

[2] *Faculdade de Engenharia de Materiais, Campus de Ananindeua, Universidade Federal do Pará, Ananindeua, Pará, Brazil*

[3] *Departmento de Engenharia de Materiais, Universidade Federal do Rio Grande do Norte, Natal-RN, Brazil*

ABSTRACT: The use of Mg-montmorillonite in the production of organoclay without sodium activation was investigated. For this purpose, organophilization experiments were carried out by varying the concentration of two surfactants: hexadecyltrimethylammonium ($HDTMA^+$) and dodecyltrimethylammonium ($DTMA^+$) ions. These surfactants were used at concentrations 0.7, 1.0 and 1.5 times that of the cation exchange capacity (62.6 meq/100 g) of the clay, with a reaction time of 8 h at temperatures of 25 and 80°C. X-ray diffraction (XRD) results confirmed the intercalation for both *in natura* and activated samples. The Fourier-transform infrared (FTIR) spectroscopy and XRD results showed that the ratio of *gauche/trans* conformers decreased with increased basal spacing. The results of thermodifferential and thermogravimetric analysis (DTA/DTG) confirmed the thermal stability of the organoclay up to 200°C, permitting the use of such material in the synthesis of polymer/clay nanocomposites obtained by the melt blending. Thus, Mg-montmorillonite can be intercalated with alkylammonium ions without prior Na-activation to form organoclays. The possibility of using natural (non-activated) Mg-montmorillonite represents a significant difference in terms of processing cost in comparison with existing Ca-montmorillonite in Brazil or even with imported bentonites that require Na-activation during beneficiation.

KEYWORDS: Mg-montmorillonite, organoclay, sodium activation, smectite, bentonite.

The process of organophilization of bentonites with alkylammonium ions has been used widely mainly because of the facility to intercalate such ions into the interlayer space of montmorillonite. Once merged, the hydrophilic character on the surface of clay minerals changes to hydrophobic and the organic-inorganic hybrid material formed exhibits chemical and physical properties of both clay minerals and organic compounds

(Lagaly *et al.* 2006; Ruiz-Hitzky & Van Meerbeek, 2006). This type of material, referred to as an organoclay, is potentially indicated for use as an adsorbent for organic pollutants (*e.g.* oil spills and their derivatives in water bodies), as rheology-control agents, as drilling mud fluids and, more recently, in the synthesis of nanocomposites (Paiva *et al.*, 2008, CMS, 2013).

In general, the interlayer space of an *in natura* montmorillonite is occupied by water molecules and cations (mainly Na^+, K^+, Mg^{2+}, Ca^{2+}), that are weakly bound to the clay-mineral layers. These cations balance the negative charge generated by isomorphic

*E-mail: manoella.cavalcante@hotmail.com

substitutions in the TOT structure of the clay mineral, which are easily replaced by cationic species external to the structure, especially in liquid medium, due to increased mobility (Moore & Reynolds, 1997; Güven, 2009; Dohrmann *et al*., 2012). This crystallochemical characteristic grants montmorillonite a large cation exchange capacity (CEC) that must be taken into account in any organophilization process, as well as the composition of exchangeable cations (McAtee *et al*., 1959; Mermut & Lagaly, 2001; He *et al*., 2010).

Bentonite – both natural and modified – is an extremely versatile clay due to the variety of properties it can exhibit in response to minor modifications in montmorillonite. Each type of bentonite meets the requirements of different specific applications according to their characteristics. Wyoming bentonite (Na-montmorillonite), for instance, is excellent for use in drilling fluids and casting but is inadequate for oil bleaching or in the manufacture of catalysts. On the other hand, bentonites from Mississippi (Ca-montmorillonite) are good for use in bleaching oils and casting but cannot be used in well drilling (Grim, 1968). For organophilization, the Wyoming type is considered to be the most suitable because Na^+ is more easily exchanged for alkylammonium ions than Ca^{2+} (Theng *et al*., 1967; Murray, 2007). However, because Na-bentonite deposits are rare, the commercially more available Ca varieties are transformed into Na-bentonites by chemical treatment with Na reagents (Na_2CO_3 is the most widely used) – a process known at the industrial level as sodium activation. The same happens at the laboratory scale where the process is used to exchange the cations in liquid phase.

The occurrence of a Mg-montmorillonite known as 'Formosa' bentonite in northeastern Brazil was described by Paz *et al*. (2012). This cationic type has not been described previously among known Brazilian bentonites occurrences and has attracted considerable attention due to the predominance of Mg in the interlayer space. This feature motivated the present work, which aimed to evaluate the feasibility of synthesizing organoclays using Formosa bentonite (Mg-montmorillonite) as the starting material, without prior Na-saturation, leading to cost savings in the synthesis process.

MATERIALS AND METHODS

Mg-montmorillonite

Approximately 40 kg of bentonite containing Mg-montmorillonite was collected from the location

described and sampled for the first time by Paz *et al*. (2012). Composite sampling was conducted at various points within the same outcrop (06°25′12″S, 46° 10′52″W), which is located next to highway MA 006, in the city of Formosa da Serra Negra, southern Maranhão State, Brazil.

At the laboratory, the initial sample (~40 kg) was dried at 60°C and homogenized, and a 5 kg sub-sample was extracted for the present study. The first step in the preparation of the material was crushing in a RETSCH jaw crusher, model BB2. The sample was then ground in an HERZOG orbital mill (*Shatter Box*), model HSM100, and sieved manually to achieve a classification size of <0.15 mm (100 Mesh). The material retained in the sieve was ground again in the orbital mill until the entire sample passed through the sieve. To ensure the homogeneity of the material, quartering was conducted according to the elongated and conical heap methods.

Surfactants

The organic salts used in the synthesis of organoclays were hexadecyltrimethylammonium bromide (HDTMA) and dodecyltrimethylammonium bromide (DTMA) (Merck Shouchardt, Germany).

Reference materials

Three reference samples were used in this study: (1) two smectite clays from the USA: SWy-2 (Na-montmorillonite; CEC: 85 meq/100 g) and SAz-1 (Ca-montmorillonite; CEC: 123 meq/100 g). They were obtained from the Source Clays Repository of The Clay Minerals Society; and (2) a commercial organoclay, Cloisite® 10A (surfactant: dimethyl, benzyl, hydrogenated tallow, quaternary ammonium), sold worldwide by Southern Clay Products, Inc.

Treatment with sodium carbonate (Na^+ activation)

For Na^+ activation, 2.5 kg of Mg-bentonite was mixed with 662.5 mL of 2 M Na_2CO_3 solution which corresponded to a CEC of 100 meq Na^+/100 g clay. The mixture was homogenized manually and aged for 7 days in a moist chamber at 100% relative humidity. The material was stirred for 1 min daily. After 7 days, the final wet product was dried at 60°C and pulverized in a mortar. The methodology described was based on the activation step carried out by those industries which specialize in the exploration for and beneficiation of

bentonite. The suffix 'Act' was added to the Na-activated sample, *i.e.* Mg-montmorillonite-Act.

Organophilization process

The variables studied are as follows: (1) *in natura* and Na-activated clays as starting materials; (2) $HDTMA^+$ and $DTMA^+$, as surfactant ions; (3) 0.7, 1.0 and $1.5 \times CEC$ of Mg-montmorillonite, as the surfactant concentration, and (d) 25 and 80°C of temperature. A summary of the experiments, along with the code used for each product is shown in Table 1.

100 g of clay was mixed with 700 mL of water in a glass reactor under vigorous mechanical agitation for 2 h. After this period, the surfactant was added and agitation of the mixture was maintained for 8 h. The clay was then washed and filtered with distilled water to remove the remaining surfactant, dried at 60°C, disaggregated manually by crushing in a mortar, sieved and homogenized to <0.15 mm.

Analyses

X-ray diffraction. The Mg-montmorillonite prepared with and without activation, the organoclays and the reference materials were examined using a PANalytical diffractometer, model X´PERT PRO MPD (PW 3040/60), with a PW3050/60 (θ/θ) goniometer, a ceramic X-ray Cu anode ($K\alpha 1 = 1.540598$ Å), with a long fine-focus (2200 W/60 kV), nickel Kβ filter, 40 kV voltage, 30 mA current, and 0.02°2θ step size. The specific conditions for each method used are shown below.
(1) For powder samples: scan range 3–70°2θ for natural and activated Mg-montmorillonite when compared with the reference smectite clays, and 2–18°2θ for organoclays, Cloisite 10A and Mg-montmorillonite with and without Na-activation; 30 s scanning time per step; fixed anti-scatter slit of 1/4°; 5 mm mask; and sample rotation of 1 revolution s^{-1}.
(2) For oriented samples in glass slides: scan range of 3–35°2θ, time/step of 10 s; divergent slit of 1/8°; anti-scatter slit of 1/4°; and 10 mm mask, without rotation. The oriented samples were X-rayed air dried, followed by ethylene glycol (EG) solvation and heating at 550°C for 2 h. The Hofmann & Klemen (1950) treatment was applied, namely Li^+ saturation, heating at 300°C for 12 h, and EG solvation.

X-ray fluorescence spectrometry. The XRF spectrometer employed was a wavelength-dispersive (WDS) sequential Axios-Minerals model (PANalytical) with a ceramic X-ray tube and a rhodium anode of maximum 2.4 kW power level. The specimens were prepared as glass discs (1 g of sample plus 6 g of lithium metaborate) using the *IQ+* program of PANalytical's SuperQ Manager. Measurements of loss on ignition (LOI) were made on independent test portions of each material by heating for 1 h at 1000°C in a muffle furnace.

Thermal analysis. The measurements were carried out on ~17 mg of sample in a PL Thermal Science STA1000/1500 simultaneous thermal analyzer (Stanton Redcroft Ltd.) with a cylindrical vertical furnace, a digital converter coupled to a microcomputer. The experiments were performed on alumina crucibles, over the temperature range of 25–1100°C, a heating rate of 20°C/min and air flow.

Exchangeable cations and cation exchange capacity. The Ca^{2+} and Mg^{2+} exchangeable cations were obtained by extraction with 1 N KCl, and were measured using EDTA as the titrant and Eriochrome Black T as the indicator. The K^+ and Na^+ exchangeable cations were obtained by extraction with Mehlich solution and were measured using a BENFER flame photometer (BFC 150 model). The CEC was defined as the sum of the exchangeable cations ($Ca^{2+} + Mg^{2+} + K^+ + Na^+$). This is the standard method used for CEC analysis by the Brazilian Agency for Agricultural Research (EMBRAPA, 1998).

Fourier transformed infrared spectroscopy. These analyses were performed on a Thermo IR100 FTIR spectrometer in the spectral range 4000–400 cm^{-1}. Each spectrum is the sum of 64 scans with 4 cm^{-1} resolution. The samples were prepared with the KBr method at a ratio of 1 mg of sample to 150 mg of KBr.

RESULTS AND DISCUSSION

Characterization of the Mg-bentonite

Identification of mineral constituents. The dominant mineral is montmorillonite, with main peaks at 1.52 nm (d_{001}), 0.445 nm (d_{100}) and 0.149 nm (d_{060}) (Fig. 1). Minor phases present are kaolinite (0.72 nm), hematite (0.270 nm and 0.251 nm), K-feldspar (0.423 nm and 0.379 nm), and anatase (0.351 nm and 0.189 nm) (Fig.1).

The XRD pattern of the oriented clay fraction (Fig. 2) contains montmorillonite, illite and kaolinite (d_{001} spacings of 1.51 nm, 1.0 nm, and 0.72 nm, respectively). Illite was not identified in the bulk

TABLE 1. Coding of organoclays.

Mg-montmorillonite	Surfactant	×CEC (meq/100 g clay)	Temperature (°C)	Code
Without Na$^+$ activation	DTMA (D)	0.7	25	0.7XD25
			80	0.7XD80
		1.0	25	1.0XD25
			80	1.0XD80
		1.5	25	1.5XD25
			80	1.5XD80
With Na$^+$ activation		0.7	25	0.7XD25-Act
			80	0.7XD80-Act
		1.0	25	1.0XD25-Act
			80	1.0XD80-Act
		1.5	25	1.5XD25-Act
			80	1.5XD80-Act
Without Na$^+$ activation	HDTMA (HD)	0.7	25	0.7XHD25
			80	0.7XHD80
		1.0	25	1.0XHD25
			80	1.0XHD80
		1.5	25	1.5XHD25
			80	1.5XHD80
With Na$^+$ activation		0.7	25	0.7XHD25-Act
			80	0.7XHD80-Act
		1.0	25	1.0XHD25-Act
			80	1.0XHD80-Act
		1.5	25	1.5XHD25-Act
			80	1.5XHD80-Act

sample due to the low concentration of this mineral (Fig. 1). After EG solvation, the 001 diffraction maximum shifted from 1.51 nm to 1.71 nm and the d_{002} reflection appeared at 0.85 nm, indicating pure smectite with no interstratification. After heating at 550°C for 2 h, the main peak of smectite shifted to 0.995 nm due to the collapse of the layer.

When montmorillonite was subjected to lithium saturation and heating, Li$^+$ cations migrated in the octahedral sheet, neutralizing the layer charge which originated from the isomorphic replacement of Al^{3+} by Mg^{2+} or Fe^{2+} and resulted in collapse of the layer, which then forms a pyrophyllite-like structure (Greene-Kelly, 1952). This behavior was observed with the Mg-montmorillonite in the present study (Fig. 2). After saturation with Li$^+$ (Hofmann & Klemen, 1950), the d_{001} value of ~0.97 nm confirmed that the smectite present was a montmorillonite, in accordance with Paz *et al*. (2012).

The XRD pattern of the Mg-montmorillonite sample was compared with Ca- and Na-montmorillonites (Fig. 1). The Mg- and Ca-montmorillonites exhibit d_{001} spacing at ~1.52 nm, and the Na-montmorillonite d_{001} spacing at 1.27 nm. According to Yildiz & Kuscu (2007), diffraction maxima at 1.48–1.55 nm indicate the presence of Ca-Mg-smectites, as in Mg-montmorillonite and SAz-1 clays, and maxima at ~1.25 nm indicate the presence of Na-montmorillonite, as in the case of SWy-2 smectite. Na-activated Ca-Mg-smectites also show $d_{001} \approx 1.25$ nm due to the exchange of the interlayer cations Mg^{2+} and/or Ca^{2+} by Na$^+$, as was observed for Mg-montmorillonite-Act (Fig. 1).

Chemical composition. The chemical composition of the Mg-montmorillonite sample and the reference samples SWy-2 and SAz-1 are shown in Table 2. SiO$_2$ and Al$_2$O$_3$ are the main constituents of all clays. The Mg-montmorillonite sample has the smallest SiO$_2$ content relative to the reference sample, probably because of the absence of quartz. The abundance of Al$_2$O$_3$ is comparable in all samples.
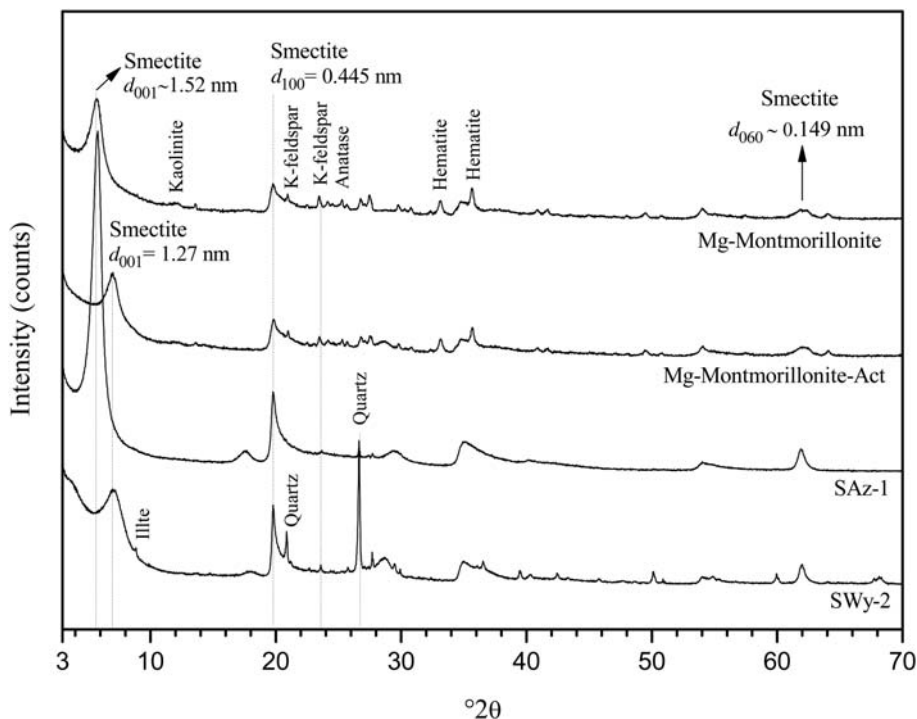
FIG. 1. Comparison of XRD patterns of the Mg-montmorillonite, with and without Na activation, with those of the SWy-2 and SAz-1 bulk samples.

The Mg-montmorillonite sample exhibits greater Fe_2O_3 contents than the reference samples, a feature that is characteristic of Brazilian bentonite clays. The explanation for this lies in the presence of hematite which influences the colour of the sample directly, imparting a reddish-brown hue. The SWy-2 and SAz-1 bentonites exhibit a greyish color.

The only sample with a relatively large Na_2O content (1.98%) was SWy-2, which represents a rare smectite clay in which Na^+ is naturally the main interlayer cation. It is therefore identified in the CMS Source Clays Repository as a Na-montmorillonite. SAz-1 has the largest CaO content (2.95%), and is known as a Ca-montmorillonite because Ca^{2+} is the main constituent in the interlayer space. Magnesium may be present both in the octahedral sheet and in the interlayer space. Typically, Mg^{2+}, as well as Fe^{2+}, is present in the octahedral sites of the montmorillonite, replacing the Al^{3+} and generating a charge imbalance (of ~0.2–0.6) in the layer, which is compensated for by the interlayer cations (Guggenheim *et al.*, 2006). In the case of the Mg-montmorillonite sample, Mg^{2+} is present both in the octahedral sheet and in the interlayer space. In this respect, Mg-montmorillonite differs from the reference clays from the USA and Brazil, which have been described in the literature as polycationic (Amorim *et al.*, 2004; Moraes *et al.*, 2010). To confirm the predominant cation present in the interlayer space, an analysis of the exchangeable cations was carried out as described in the following subsection. The greater TiO_2 and K_2O contents in the Mg-montmorillonite sample, in comparison with those of SWy-2 and SAz-1, are mainly related to the presence of anatase and K-feldspar as accessory minerals in the clay.

The results of the chemical analysis carried out in this study were compared with the results of Paz *et al.* (2012) for Mg-montmorillonite and of Mermut & Cano (2001) for SAz-1 and SWy-2. The values obtained in the present study are comparable to those reported in the literature.

Composition of exchangeable cations and cation exchange capacity. The composition of the exchangeable cations of the Mg-montmorillonite sample and the CEC showed that Mg^+ is the predominant exchangeable cation, confirming its cationic type (Table 3). The CEC value of Mg-montmorillonite (62.6 meq/100 g)
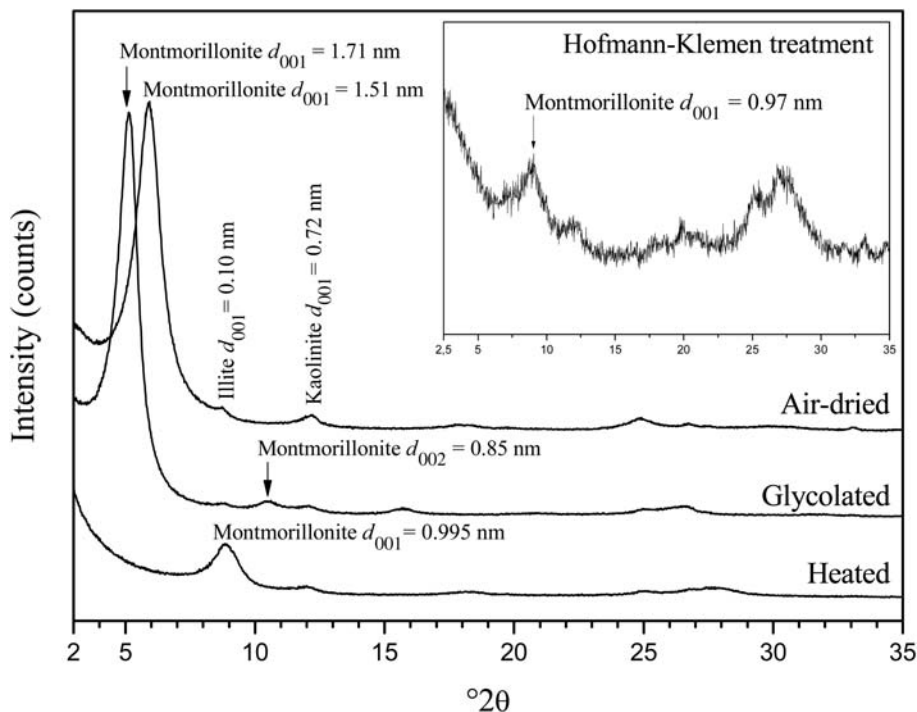
FIG. 2. XRD patterns of the oriented <2 mm fraction of the Mg-montmorillonite after air-drying, glycolation, heating at 550°C and Hofmann-Klemen treatment.

was less than for Na-montmorillonite (85 meq/100 g) and Ca-montmorillonite (123 meq/100 g), both from Borden & Giese (2011), even when compared with the reference value of 74.8 meq/100 g obtained by Paz et al. (2012), which used the ammonium acetate method, while in this work 'KCl + Mehlich' was used. The CEC value is important in the calculation of the surfactant-ion concentration used in the synthesis of organoclays, because the quantitative exchange requires a certain excess of alkylammonium salts in relation to the CEC (Lagaly et al., 2006). In this case, three concentration values were used as follows: 0.7, 1.0, and 1.5 × 62.6 (CEC of Mg-montmorillonite obtained in this work), with the main objective of comparing the products obtained from the two cationic types (magnesian and Na-activated).

Organoclays

The XRD patterns of organoclays showed that the variation of basal-spacing values (d_{001}) of Mg-montmorillonite in natural and Na-activated forms reflect directly the type and concentration of the surfactant (Figs 3, 4). The basal spacing of

the organophilic smectite results from the sum of the following components: (1) thickness of the clay mineral layer (0.96 nm); (2) the height of the polar end of the organic cation; and (3) the number of layers of the organic species. For example, the molecular conformation of $HDTMA^+$ can exhibit two values (0.51 or 0.67 nm), depending upon the height of the polar end, if perpendicular or parallel to the montmorillonite layers (Harris et al., 1999; He et al., 2006; Hu et al. 2013) (Fig. 5). Thus, a monolayer intercalation results in a d_{001} of 1.47 nm (perpendicular) or d_{001} of 1.63 nm (parallel).

According to Lagaly et al. (2006), short-chain alkylammonium ions are arranged in monolayers, while longer chain are arranged in bilayers with the alkyl chain axes parallel to montmorillonite layers. Monolayers and bilayers exhibit basal spacings of ~1.4 nm and ~1.8 nm, respectively. Intermediate ~1.6 nm spacing may indicate mixed layering of monolayer and bilayer complexes. Therefore, according to the aforementioned models for the arrangements of the alkylammonium ions in the montmorillonite interlayers (Lagaly et al., 2006; Hu et al., 2013), the organophilic products obtained in this work can be

TABLE 2. Elemental composition of Mg-montmorillonite, SWy-2 and SAz-1.

(wt.%)	Mg-montmorillonite		SWy-2		SAz-1	
	This work	Paz *et al.* (2012)	This work	Mermut & Cano (2001)	This work	Mermut & Cano (2001)
SiO_2	48.10	48.13	63.74	61.46	60.76	59.65
TiO_2	1.16	1.49	0.13	0.09	0.19	0.25
Al_2O_3	18.66	17.40	18.80	22.05	17.24	19.98
Fe_2O_3	12.65	14.08	3.73	4.37	1.44	1.77
CaO	0.31	0.27	0.47	1.18	2.95	3.15
MgO	3.88	3.73	2.24	2.94	5.88	6.76
MnO	0.14	0.17	–	–	0.08	–
K_2O	1.56	1.59	0.64	0.20	0.16	0.19
Na_2O	–	–	1.98	1.47	–	0.06
P_2O_5	0.02	0.05	0.05	–	0.03	–
LOI	13.50	13.08	7.23	5.76	11.27	8.17
Total	99.98	99.89	99.01	99.52	100	99.98

LOI: Loss on ignition as determined by heating at 1000°C after drying at 105°C; –: below detection limit.

discussed as follows: all organoclays with $0.7 \times DTMA^+$ concentration showed $d_{001} \approx 1.45$ nm which indicates a monolayer structural arrangement (Fig.6a) (Lagaly *et al.,* 2006), with molecular conformation perpendicular to the smectite layer. The temperature and Na^+-for-Mg^{2+} exchange did not affect the structural arrangement type.

The $1.0 \times D25$ organoclay showed a broad diffraction band which can be related to two peaks (1.45 and 1.61 nm, approximately), indicating the possible coexistence of monolayer arrangements with perpendicular and parallel conformation in the montmorillonite interlayer (Harris *et al.*, 1991; He *et al.*, 2006; Hu *et al.*, 2013). Alternatively, the peak at 1.61 nm alone may indicate monolayer/bilayer transition (Lagaly *et al.*, 2006). The remaining samples with $1.0 \times DTMA$ (Fig.3) display a bilayer arrangement because they showed a d_{001} value between 1.84 and 1.96 nm (Fig. 6b).

The organoclays with $1.5 \times DTMA^+$ obtained from the synthesis conditions studied are exhibited in Fig. 3. Three organoclays showed $d_{001} \approx 2.0$ nm, even when the temperature and the cationic conditions of the starting clay varied. This may be a pseudotrilayer conformation (Fig. 6d) according to Lagaly *et al.* (2006). Only one organoclay with $1.5 \times DTMA^+$ showed a smaller d_{001} value (1.82 nm), also indicating a bilayer arrangement.

The XRD patterns of the organoclay with $0.7 \times$ concentration of $HDTMA^+$ surfactant exhibited $d_{001} \approx$ 1.62 nm (Fig. 4) indicating the presence of a monolayer

arrangement with parallel molecular conformation or mixed layering of monolayer and bilayer, as mentioned before for the organoclays obtained from $DTMA^+$. The variation of temperature as well as the type of exchangeable ions in the interlayer space do not influence the type of structural arrangement of the organoclay.

The samples $1.0 \times HD25$ and $1.5 \times HD25$-Act showed peak values of ~1.96 nm which represent bilayer arrangement. The remaining samples showed $d_{001} > 2.2$ nm suggesting paraffin-type arrangement. In this type, the organic compounds are inclined and the angles vary according to the charge or the packing density of the layer (Fig. 6e,f) (Beneke & Lagaly, 1981).

The angle of inclination (α) in paraffin-type arrangements can be calculated using the following equation: $\sin\alpha = (d-h)/l$, where d is the basal spacing, h is the layer thickness (0.96 nm) and l is the length of the organic ion chain (in the case of HDTMA = 2.53 nm) (Mermut & St Arnaud, 1990; Mermut, 1994; Hu *et al.*, 2013). The tilting angle for organoclays with values between 2.3 and 2.4 nm is ~32–35°. For those with $d_{001} \approx 2.7$ nm, the angle is ~44° (Fig. 6f).

Note that in previous studies of the synthesis of organoclays, Na-montmorillonite or Na-activated bentonite were used (Lee & Lee, 2004; Xi *et al.*, 2005; Zhou *et al.*, 2007; Nikolaidis *et al.*, 2012; Filippi *et al.*, 2013; Tsai *et al.*, 2013). Since the 1960s, it has been largely considered that this type is more effective than Ca-montmorillonite (Theng *et al.*, 1967). In the present study, organoclays derived from Mg-montmorillonite were obtained with similar characteristics to

TABLE 3. Composition of exchangeable cations and total CEC of the Mg-montmorillonite.

Mg-bentonite	Experimental method	Mg²⁺	Ca²⁺	Na⁺	K⁺	CEC (meq/100 g of clay)
		Mg^{2+}	Ca^{2+}	Na^+	K^+	
This work	KCl + Mehlich	47.5	8.5	5.3	1.3	60.6
Paz *et al.* (2012)	Ammonium acetate	60.2	9.9	3.3	1.4	74.8

those obtained after Na-activation, even when produced at different temperatures.

The variation in the d_{001} spacing can be related to the chain length of organic cations (the DTMA⁺ ion presents 12 carbon atoms while HDTMA⁺ has 16 carbon atoms) and packing density. Moreover, the organoclays synthesized with 1.0× and 1.5× the CEC (D and HD) exhibited d_{001} spacing similar to 10A Cloisite (Table 4).

Conformational identification of intercalated organic compounds

In all organoclays intercalated with DTMA⁺ and HDTMA⁺, the presence of FTIR absorption bands at 2800–3000 cm⁻¹ and 1400–1600 cm⁻¹ was observed (Figs 7, 8).

The bands at ~2920 cm⁻¹ and ~2850 cm⁻¹ originate from the asymmetric (υ_{as}) and symmetric (υ_s) stretching of –CH₂ bonds of the amine chain, respectively (He *et al.*, 2004; Fatimah & Huda, 2013). These bands, in particular υ_{as}, are extremely sensitive to conformational changes in the alkyl chains of amine (Vaia *et al.*, 1994; Xi *et al.*, 2005; Zhou *et al.*, 2007; Ma *et al.*, 2010) and bands appear in this region only when the alkyl chains are highly ordered (all with *trans* conformations). This is due to increased packing density enabling greater ordination of surfactant with *trans* conformation in the interlayer (Vaia *et al.* 1994).

A decrease in the frequency of the asymmetric stretching band with increasing surfactant concentration as well as with increasing chain length (HDTMA⁺ > DTMA⁺) was observed (Table 5). This suggests that increased packing density favours *trans*-type ordered conformations, which allows structural arrangements involving greater basal spacing. In addition, all organoclays exhibited υ_{as} values similar to those of Cloisite 10A.

Correlation of the FTIR (υ_{as}) and XRD (d_{001}) results showed that the decreased frequency of asymmetric stretching, which is associated with an increase in *trans*
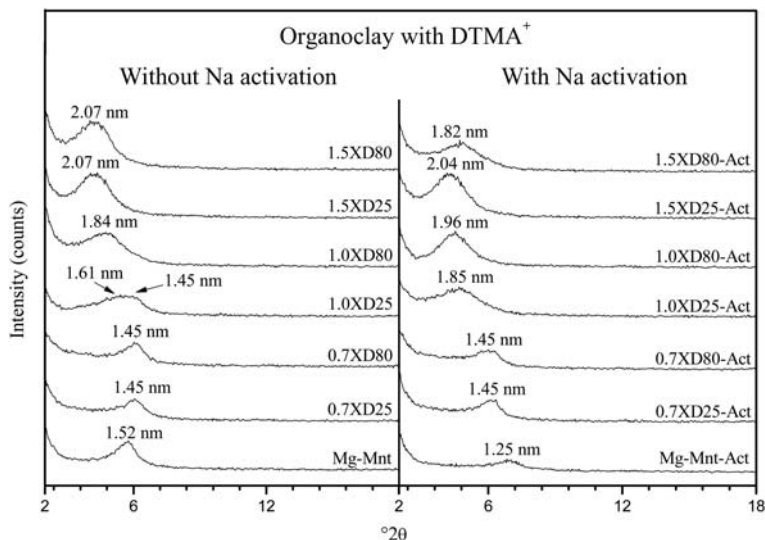

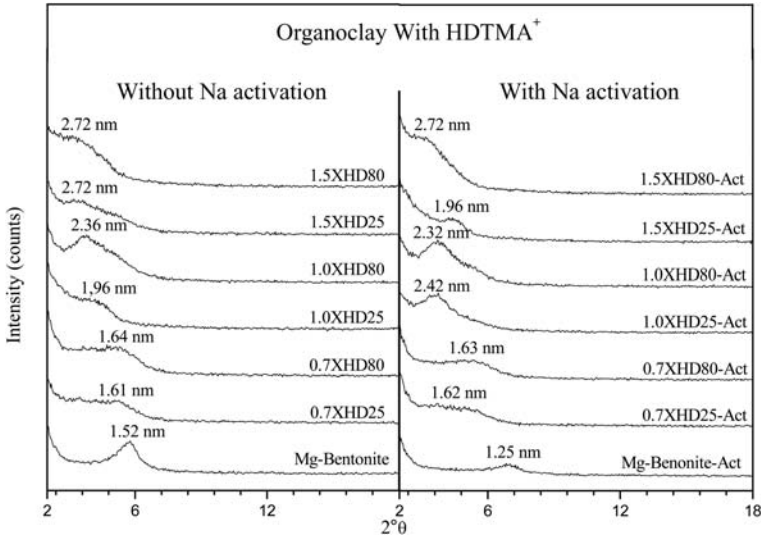FIG. 3. XRD patterns with d_{001} of organoclays with DTMA⁺.

Fɪɢ. 4. XRD patterns with d_{001} of organoclays with HDTMA$^+$.

conformation, is correlated with larger basal spacings of the organoclays. This confirms the foregoing interpretation of the structural arrangements present in the organoclay products.

The singlets present in the 1400 cm^{-1} to 1600 cm^{-1} region (Figs 7, 8) are related to the liquid-like molecular structure or disordered hexagonal packing of the material (Weers *et al.,* 1990; Zhu *et al.,* 2005). With increasing packing density and surfactant ion concentration, this singlet tends to form two scissoring vibrations (δ). This is observed in all organoclays and more intensely in Cloisite 10A. The singlets are sensitive to interactions of the amine molecules within the alkyl chain and to the type of structural arrangement. Thus, when the first band exhibits frequency variation in the range 1466–1472 cm^{-1}, there is increased ordering (all *trans* conformation) of the alkyl chains of the amine.

Conversely, bands of low frequency and decreased intensity indicate weaker interaction and greater movement of the ionic bonds. The second frequency at 1487 cm^{-1} tends to decrease with increased ordering; this is observed in clays intercalated with the two surfactants used (Zhu *et al.*, 2005).

Thermal stability

Due to the low temperature of decomposition of the intercalated organic ions, the thermal stability of organoclays is one of the major problems in the preparation of nanocomposites by fusion (Hedley *et al.* 2007).

Three main regions are observed, indicated as a, b and c in Fig. 9: the first corresponds to endothermic water desorption; the second, with two peaks,
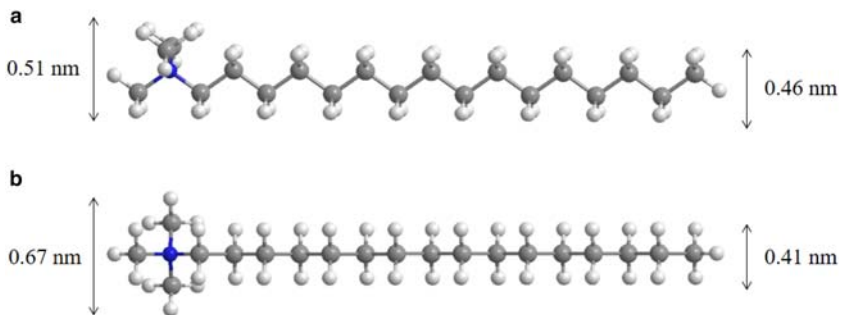

Fɪɢ. 5. Molecular conformation of HDTMA$^+$: (a) plane perpendicular to the plane of the montmorillonite layer; (b) plane parallel to the plane of the montmorillonite layer.
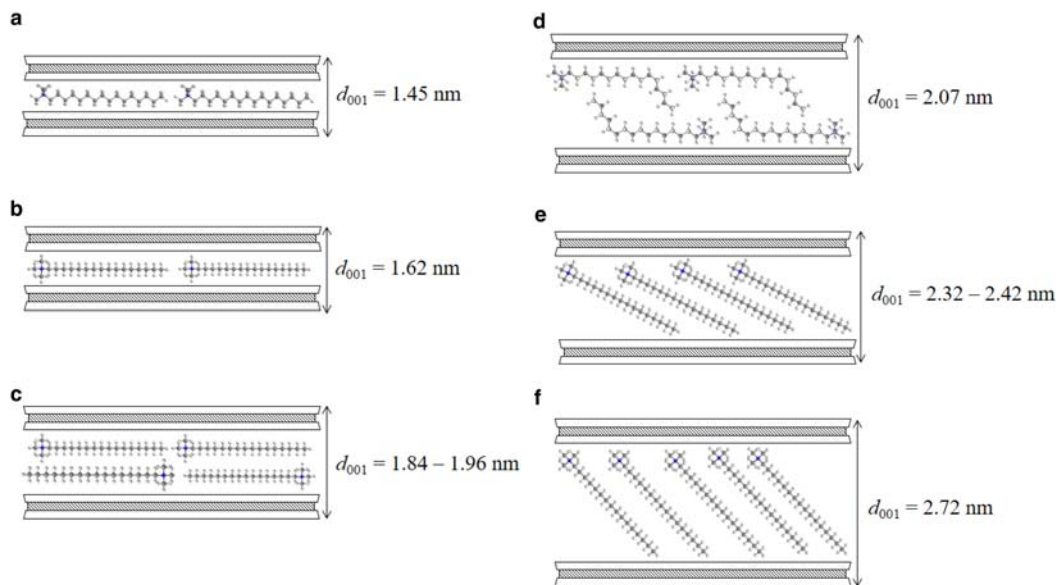
FIG. 6. Orientations of alkylammonium ions in the basal spacing of silicates: (a) monolayer with perpendicular conformation; (b) monolayer with parallel conformation; (c) bilayer; (d) pseudotrilayer; and (e,f) paraffin-type arrangements of alkylammonium ions with different tilting angles of the alkyl chains.

corresponds to the decomposition of the quaternary ammonium salt, which is exothermic; and the third is ascribed to the release of carbonaceous residues from the montmorillonite interlayer space. Delbem *et al.* (2010) observed similar behaviour in organoclays produced from bentonites from Paraíba State, Brazil.

Region a shows an inverse relationship between the amount of water desorbed from inorganic cations and the amount of water removed from the intercalated organic cations. This is because the greater the change in polarity of the interlayer species, the greater the consequent change in the character of the clay from

TABLE 4. Alkyl-chain arrangements in the interlayer space of the Mg-montmorillonite.

Organoclay without Na activation	d_{001}	Alkyl chain arrangement	Organoclay with Na activation	d_{001}	Alkyl chain arrangement
0.7XD25	1.45	Monolayer	0.7XD25-Act	1.45	Monolayer
0.7XD80	1.45		0.7XD80-Act	1.45	
0.7XHD25	1.61		0.7XHD25-Act	1.62	
0.7XHD80	1.64		0.7XHD80-Act	1.63	
1.0XD25	1.45 and 1.61	Monolayer/Bilayer	1.0XD25-Act	1.85	Bilayer
1.0XD80	1.84	Bilayer	1.0XD80-Act	1.95	
1.0XHD25	1,96		1.0XHD25-Act	2.42	Paraffin
1.0XHD80	2.36	Paraffin	1.0XHD80-Act	2.32	
1.5XD25	2.07	Pseudotrilayer	1.5XD25-Act	2.04	Pseudotrilayer
1.5XD80	2,07		1.5XD80-Act	1.82	Bilayer
1.5XHD25	2.72	Paraffin	1.5XHD25-Act	1.96	
1.5XHD80	2.72		1.5XHD80-Act	2.72	Paraffin
Cloisite 10A	1.99	–			

TABLE 5. Frequency values of the asymmetric stretching bands of organoclays.

Organoclay without Na activation	ν_{as} (cm^{-1})	Organoclay with Na activation	ν_{as} (cm^{-1})
0.7XD25	2926	0.7XD25-Act	2926
0.7XD80	2926	0.7XD80-Act	2926
1.0XD25	2926	1.0XD25-Act	2925
1.0XD80	2925	1.0XD80-Act	2924
1.5XD25	2925	1.5XD25-Act	2924
1.5XD80	2925	1.5XD80-Act	2925
0.7XHD25	2920	0.7XHD25-Act	2920
0.7XHD80	2920	0.7XHD80-Act	2920
1.0XHD25	2919	1.0XHD25-Act	2919
1.0XHD80	2919	1.0XHD80-Act	2919
1.5XHD25	2918	1.5XHD25-Act	2919
1.5XHD80	2918	1.5XHD80-Act	2918
Cloisite 10A	2923		

hydrophilic to hydrophobic, the greater is the effectiveness of the organophilization and the less solvated water is present (Guggenheim & Koster van Groos, 2001: Xie *et al.*, 2001; Paz *et al.*, 2012). The TG results for the organoclays revealed a significant decrease in water loss in this region relative to the amount of Mg-montmorillonite (9.86%; Paz *et al.* 2012); similar results were obtained for Cloisite 10A (Tables 6, 7).
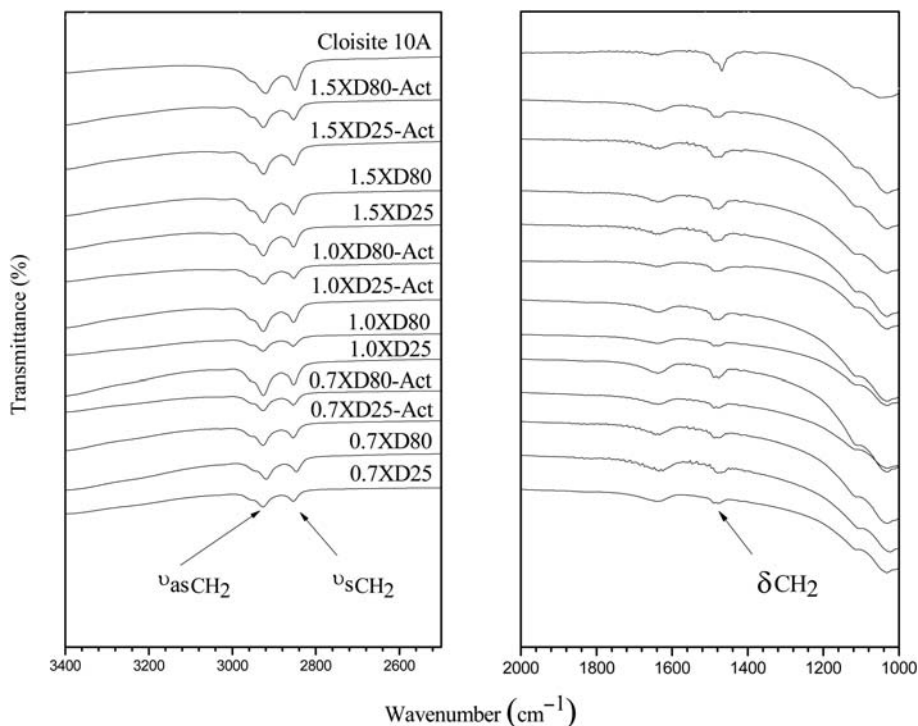
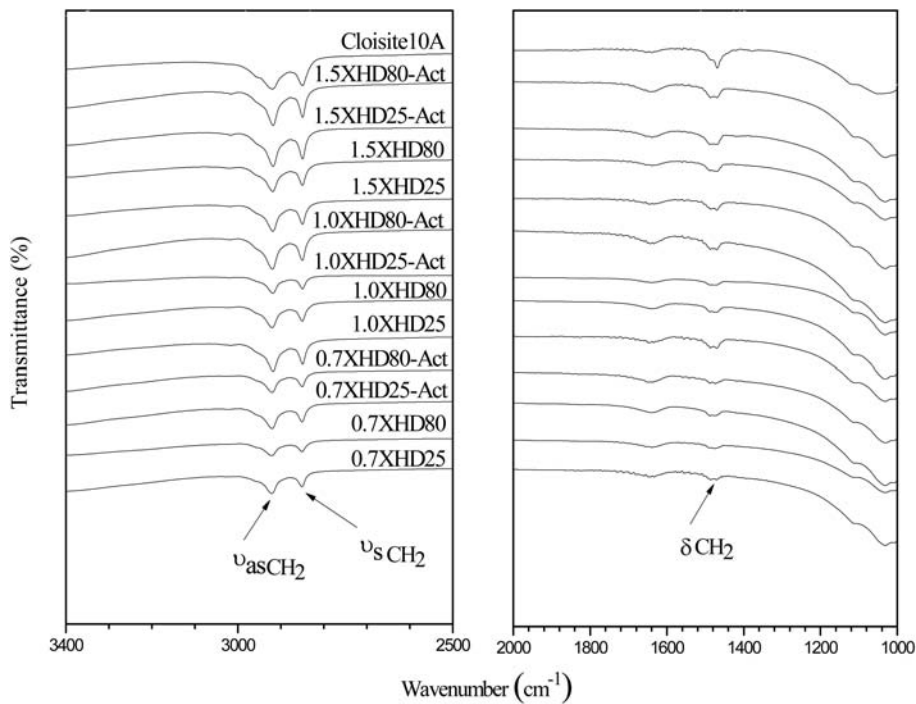FIG. 7. FTIR spectra of organoclays with DTMA^{+} and cloisite 10A.

FIG. 8. FTIR spectra of organoclays with HDTMA$^+$ and cloisite 10A.
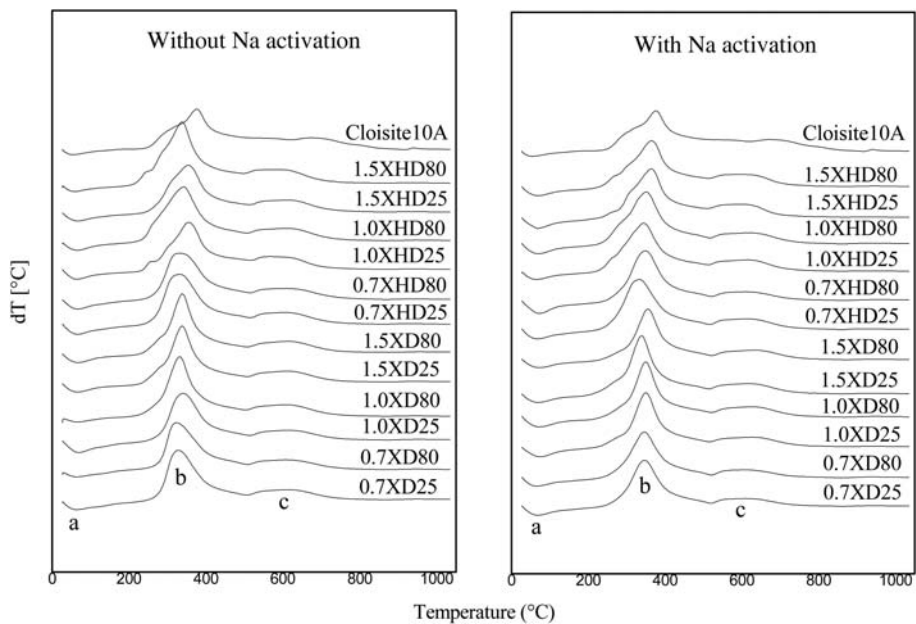

FIG. 9. DTA diagrams of organoclays with DTMA$^+$ and HDTMA$^+$ and cloisite 10A.

TABLE 6. Weight loss, determined by TG, of organoclays without Na activation and with intercalated $DTMA^+$ and $HDTMA^+$.

Organoclay without Na activation	Water loss (%) (20–200°C)	Mass loss of surfactant (%) (200–800°C)	Residual organics (%)	Total mass loss (%)
	Region (a)	Region (b)		
Cloisite 10A	3.38		0.87	41.97
0.7XD25	5.35	10.14	0.53	19.44
0.7XD80	4.15	10.93	0.21	19.16
1.0XD25	5.84	11.20	0.39	21.25
1.0XD80	3.87	13.50	0.33	21.58
1.5XD25	4.79	16.49	0.16	25.33
1.5XD80	5.04	16.56	0.40	25.73
0.7XHD25	5.38	14.36	0.40	23.9
0.7XHD80	5.45	13.89	0.52	23.68
1.0XHD25	4.58	23.93	0.28	32.70
1.0XHD80	5.18	15.94	0.39	25.32
1.5XHD25	4.26	16.46	0.13	24.81
1.5XHD80	4.86	23.62	0.18	32.00

In region b, mass loss was observed to range from 10.14 to 23.83% (Tables 6, 7). The percentages of mass loss of the surfactant were estimated subtracting the mass loss of Mg-montmorillonite, from 200 to 800°C, due to dehydroxylation, from the total mass loss of the organoclays, from 200 to 850°C (Hedley *et al.,* 2007). The Δm was greater for those products with more effective organic ion intercalation, and greater for

TABLE 7. Weight loss, determined by TG, of organoclays with Na activation, and intercalated $DTMA^+$ and $HDTMA^+$.

Organoclay with Na^+ activation	Water loss (%) (20 to 200°C)	Mass loss of surfactant (%) (200°C to 800°C)	Residual organics (%)	Total mass loss (%)
	Region (a)	Region (b)		
Cloisite 10A	3.38		0.87	41.97
0.7XD25	4.51	10.93	0.37	19.62
0.7XD80	4.09	10.77	0.26	18.89
1.0XD25	3.74	12.05	0.28	21.04
1.0XD80	5.27	15.94	0.39	25.42
1.5XD25	4.65	15.14	0.26	23.75
1.5XD80	4.74	12.89	0.32	21.84
0.7XHD25	5.65	13.17	0.39	22.75
0.7XHD80	5.38	12.71	0.27	22.36
1.0XHD25	4.95	17.75	0.32	26.60
1.0XHD80	4.80	16.88	0.24	25.73
1.5XHD25	3.93	23.83	0.19	31.78
1.5XHD80	4.68	23.01	0.22	31.76

species with larger molecular weight ($HDTMA^+ >$ $DTMA^+$). In region b, there is also a tendency for the formation of a second exothermic peak in the organoclays produced. This second peak is characteristic of organoclays containing high concentrations of organic ions (He *et al.*, 2005).

Region c corresponds to products associated with residual organic carbon. The higher the salt concentration, the greater the amount of residue produced by the organoclay. This is of great importance for the synthesis of nanocomposites because this residue may act as a flame retardant (Yariv, 2004; Carrado & Komadel, 2009).

All organoclays intercalated with $DTMA^+$ and $HDTMA^+$ showed very similar carbon residue values (<1%) (Tables 6, 7), suggesting that the concentration of the organic salt (0.7, 1.0 and 1.5) has no influence.

CONCLUSIONS

The Mg-montmorillonite described here can be used for synthesis of organophilic clays both in the activated and the natural forms. The synthetic organoclays that yielded the best results in this study were those intercalated with $HDTMA^+$. For most of the synthesis conditions used here, natural Mg-montmorillonite gave a greater yield of intercalated organic ions than Na-activated montmorillonite. This finding is of economic interest in the industry because it eliminates one step in the synthesis process.

REFERENCES

Amorim L.V., Gomes C.M., Lira H.L., França K.B. & Ferreira, H.C. (2004) Bentonites from Boa Vista, Brazil: physical, mineralogical and rheological properties. *Materials Research*, **7**, 583–593.

Beneke K. & Lagaly G. (1982) The brittle mica-like $KNiAsO_4$ and its organic derivatives. *Clay Minerals*, **17**, 175–183.

Borden D. & Giese, R.F. (2001) Baseline studies of the Clay Minerals Society Source Clays: Cation exchange capacity measurements by the ammonia-electrode method. *Clays and Clay Minerals, 49*, **5**, 444–445.

Carrado K.A. & Komadel P. (2009) Acid activation of bentonites and polymer–clay nanocomposites. *Elements*, **5**, 93–98.

Clay Minerals Society (CMS) (2013) Glossary for Clay Science Project. http://www.clays.org/GLOSSARY/ GlossIntro.html.

Delbem M.F., Valera T.S., Valenzuela-Diaz F.R. & Demarquette, N.R. (2010) Modification of a Brazilian smectite clay with different quaternary ammonium salts. *Química Nova, 33*, **2**, 309–315.

Dohrmann R., Genske D., Karnland O., Kaufhold S., Kiviranta L., Olsson S., Tze M.P., Sandén, T, Sellin P., Svensson D. & Valter A., (2012) Interlaboratory CEC and exchangeable cation study of bentonite buffer materials: I. Cu(II)-triethylenetetramine method. *Clays and Clay Minerals*, **60**, 2, 162–175.

EMBRAPA – Brazilian Agricultural Research Corporation. (1998) Manual de Métodos de Análises de Solo. Ministry of Agriculture, Livestock and Food Supply.

Fatimah I. & Huda T. (2013) Preparation of cetyltrimethyl-ammonium intercalated Indonesian montmorillonite for adsorption of toluene. *Applied Clay Science*, **74**, 115–120.

Filippi S., Paci M., Rossi F.B.D. & Polacco G. (2013) XRD study of intercalation in statically annealed composites of ethylene copolymers and organically modified montmorillonites. *1. Two-tailed organo-clays. Journal of the Taiwan Institute of Chemical Engineers*, **44**, 123–130.

Greene-Kelly R. (1952) Irreversible dehydration in montmorillonite, *Clay Minerals Bulletin, 1*, 221.

Grim, R.E. (1968) *Clay Mineralogy.* McGraw-Hill Book Co. Inc., New York. 596 pp.

Guggenheim S., Adams J.M., Bain D.C., Bergaya F., Brigatti M.F., Drits V.A., Formoso, M.L.L., Galán E., Kogure T. & Stanjek H. (2006) Summary of recommendations of nomenclature committees relevant to clay mineralogy: report of the Association Internationale Pour l'Etude des Argiles (AIPEA) nomenclature committee. *Clays and Clay Minerals*, **54**, 761–772.

Guggenheim S., Van K. & Gross, A.F. (2001) Baseline studies of the Clay Minerals Society Source Clays: Thermal analysis. *Clays and Clay Minerals*, **49**, 433–443.

Güven N. (2009) Bentonite – clays for molecular engineering. *Elements*, **5**, 89–92.

Harris D.J., Bonagamba T.J. & Schmidt-Rohr K. (1999) Conformation of poly(ethylene oxide) intercalated in clay and MoS_2 studied by two-dimensional double-quantum NMR. *Macromolecules*, **32**, 6718–6724.

He H., Frost R.L., Bostrom T., Yuan P., Duong L., Yang D., Xi Y. & Kloprogge J.T. (2006) Changes in the morphology of organoclays with HDTMA$^+$ surfactant loading. *Applied Clay Science*, **31**, 262–271.

He H., Frost. R. & Zhu J. (2004) Infrared study of HDTMA+ intercalated montmorillonite. *Spectrochimica Acta, Part A*, **60**, 2853–2859.

He H.P., Ding Z., Zhu J.X., Yuan P., Xi Y.F., Yang D. & Frost, R.L. (2005) Thermal characterization of surfactant-modified montmorillonites. *Clays and Clay Minerals*, **53**, 286–292.

He H.P., Ma Y.H., Zhu J.X., Yuan P. & Qing, Y.H. (2010) Organoclays prepared from montmorillonites with different cation exchange capacity and surfactant configuration. *Applied Clay Science*, **48**, 67–72.

Hedley C.B., Yuan G.B. & Theng K.G. (2007) Thermal analysis of montmorillonites modified with quaternary phosphonium and ammonium surfactants. *Applied Clay Science*, **35**, 180–188.

Hofmann U. & Klemen E. (1950) Loss of exchangeability of lithium ions in bentonite on heating. *Zeitschrift für Anorganishe und Allgemeine Chemie*, **262**, 95–99.

Hu Z., He G., Liu Y., Dong C., Wu X. & Zhao W. (2013) Effects of surfactant concentration on alkyl chain arrangements in dry and swollen organic montmorillonite. *Applied Clay Science,* 75–76, 134–140.

Lagaly G. (1986) Interaction of alkylamines with different types of layered compounds. *Solid State Ionics*, **22**, 43–51.

Lagaly G., Ogawa M. & Dékány I. (2006) Clay mineral organic interactions. Pp. 309–377 in: *Handbook of Clay Science* (F. Bergaya, B.K.G. Theng, & G. Lagaly, editors). Developments in Clay Science, **1**, Elsevier, Amsterdam.

Lee J.Y. & Lee, H.K. (2004) Characterization of organobentonite used for polymer nanocomposites. *Materials Chemistry and Physics*, **85**, 410–415.

Ma Y., Zhu J., He H., Yuan P., Shen W. & Liu D. (2010) Infrared investigation of organo-montmorillonites prepared from different surfactants. *Spectrochimica Acta Part A.* **76,** 122–129.

McAtee, J.L. (1959) Inorganic-organic cation exchange on montmorillonite. *American Mineralogist*, **44**, 1230–1236.

Mermut A.R. & Lagaly G. (2001) Baseline studies of the Clay Minerals Society Source Clays: Layer-charge determination and characteristics of those minerals containing 2:1 layers. *Clays and Clay Minerals*, **49**, 393–397.

Mermut A.R. (1994) Problems associated with layer charge characterization of phyllosilicates. Pp. 106–122 in: *Layer Charge Characteristics of Clays*, (A.R. Mermut, editor). CMS Workshop Lectures, **6**, The Clay Minerals Society, Boulder, Colorado, USA.

Mermut A.R. & Cano, A.F. (2001) Baseline studies of the clay minerals society source clays: Chemical analyses of major elements. *Clays and Clay Minerals,* **49**, 381–386.

Mermut A.R. & St. Arnaud, R.J. (1990) Layer charge determination of high charge phyllosilicates by alkylammonium technique. 27th Annual Meeting of the Clay Minerals Society, Columbia, Missouri, Program and Abstracts, p. 86.

Moore D.M. & Reynolds, Jr. R.C. (1997) *X-ray Diffraction and the Identification of Clay Minerals.* Oxford University Press, New York.

Moraes D.S., Angélica R.S., Costa, C.E.F., Rocha Filho G.N. & Zamian, J.R. (2010) Mineralogy and chemistry of a new bentonite occurrence in the eastern Amazon region, northern Brazil. *Applied Clay Science*, **48**, 475–480.

Murray, H.H. (2007) *Applied Clay Mineralogy: Occurrences, Processing and Application of Kaolins, Bentonites, Palygorskite-Sepiolite, and Common Clays*. Elsevier, Amsterdam, pp. 111–130.

Nikolaidis A.K., Achilias D.S. & Karayannidis G.P. (2012) Effect of the type of organic modifier on the polymerization kinetics and the properties of poly (methyl methacrylate)/organomodified montmorillonite nanocomposites. *European Polymer Journal*, **48**, 240–251.

Paiva L.B., Morales A.R. & Díaz F.R.V. (2008) Na overview on organophilic clays: properties, routes of preparation and applications. *Applied Clay Science*, **42**, 8–24.

Paz S.P.A., Angélica R.S. & Neves R.F. (2012) Mg-bentonite in the Parnaíba Paleozoic Basin, northern Brazil. *Clays and Clay Minerals, 60*, **3**, 265–277.

Ruiz-Hitzky E. & Van Meerbeek A. (2006) Clay mineral and organoclay–polymer nanocomposites Pp. 583–622 in: *Handbook of Clay Science* (F. Bergaya, B.K.G. Theng, & G. Lagaly, editors). Developments in Clay Science, **1**, Elsevier, Amsterdam.

Theng, B.K.G., Greenland, D.J. & Quirk, J.P. (1967) Adsorption of alkylammonium cations by montmorillonite. *Clay Minerals,* **7,** 1–17.

Tsai, T.-Y., Lin, M.-J., Chuang, Y.-C. & Chou, P.-C. (2013) Effects of modified clay on the morphology and thermal stability of PMMA/clay nanocomposites. *Materials Chemistry and Physics,* **138,** 230–237.

Vaia R.A., Teukolsky R.K. & Giannelis, E.P. (1994) Interlayer structure and molecular environment of alkylammonium layered silicates. *Chemistry of Materials*, **6**, 1017–1022.

Weers J.G. & Scheuing, D.R. (1990) In Fourier Transform Infrared Spectroscopy in Colloid and Interface Science (D.R. Scheuing, editor); ACS Symposium Ser. 447, American Chemical Society, Washington, DC.

Wen X., He H., Zhu J., Juna Y., Ye C. & Denga F. (2006) Arrangement, conformation, and mobility of surfactant molecules intercalated in montmorillonite prepared at different pillaring reagent concentrations as

studied by solid-state NMR spectroscopy. *Journal of Colloid and Interface Science*, **29**, 754–760.

Xi Y., Ding Z., He H. & Frost R.L. (2005) Infrared spectroscopy of organoclays synthesized with the surfactant octadecyltrimethylammonium bromide. *Spectrochimica Acta Part A*, **61**, 515–525.

Xie W., Gao Z., Pan, W-P., Hunter D., Singh A. & Vaia, R. (2001) Thermal degradation chemistry of alkyl quaternary ammonium montmorillonite. *Chemistry of Materials*, **13**, 2979–2990.

Yariv S. (2004) The role of charcoal on DTA curves of organo-clay complexes: an overview. *Applied Clay Science*, **24**, 225–236.

Yildiz A. & Kuscu M. (2007) Mineralogy, chemistry and physical properties of bentonites from Baören, Kütahya W. Anatolia, Turkey. *Clay Minerals*, **42**, 399–414.

Zhou Q., Frost R.L., He H., Xi Y. & Liu H. (2007) Adsorbed para-nitrophenol on HDTMAB organoclay—A TEM and infrared spectroscopic study. *Journal of Colloid and Interface Science*, **307**, 357–363.

Zhu J., He H., Zhu L., Wen X. & Deng F. (2005) Characterization of organic phases in the interlayer of montmorillonite using FTIR and ^{13}C NMR. *Journal of Colloid and Interface Science*, **286**, 239–244.